

Orientation Tuning in Visual Cortex and the “Ring” Model of Cortical Gain

An interested puzzle is posed by the response of neurons in V1 cortex to oriented bars or drifting and oriented grating. Different cells respond to different angles, with a width and baseline to the response. This defines the tuning curve. The same cells also respond to the contrast of the scene; at high light levels the contrast and not the absolute intensity determines the average spike rate while the contrast determines the modulation of the rate so long as the modulation is not too slow or too fast.

Two conundrums, summarized in the Current Opinions in Neurobiology article by Shapley and Sompolinsky, arise:

- (1) The width of the tuning curve is independent of contrast. This appears to be inconsistent with feed forward models, in which a fixed threshold would cause the width to increase with increasing contrast.
- (2) The width of the tuning curve is largely independent of the aspect ratio of the oriented bar. For small bars, this is inconsistent with a geometrically-based feed forward model, *i.e.*, the Hubel-Wiesel Model.

Let's see if a recurrent network with input broadly tuned to orientation can have positive feedback to surmount these challenges. In the sense, the stable states of the network are now features, *i.e.*, preferred orientations of edges in the visual field, as opposed to abstract memories

I. The model

We have N neurons, each with a preferred angle θ_i for different stimuli, where $0 < \theta_i < \pi$. Thus:

$$(1) \quad \theta_i = \frac{\pi}{N} i \quad \forall_i .$$

We hypothesize, consistent with the results of experiment, that the weights of the synaptic connections between neurons is of the form

$$(2) \quad W_{ij} = \frac{1}{N} J(\theta_i - \theta_j)$$

which follows from the functional and anatomical data for neurons in cat V1 (see Figures).

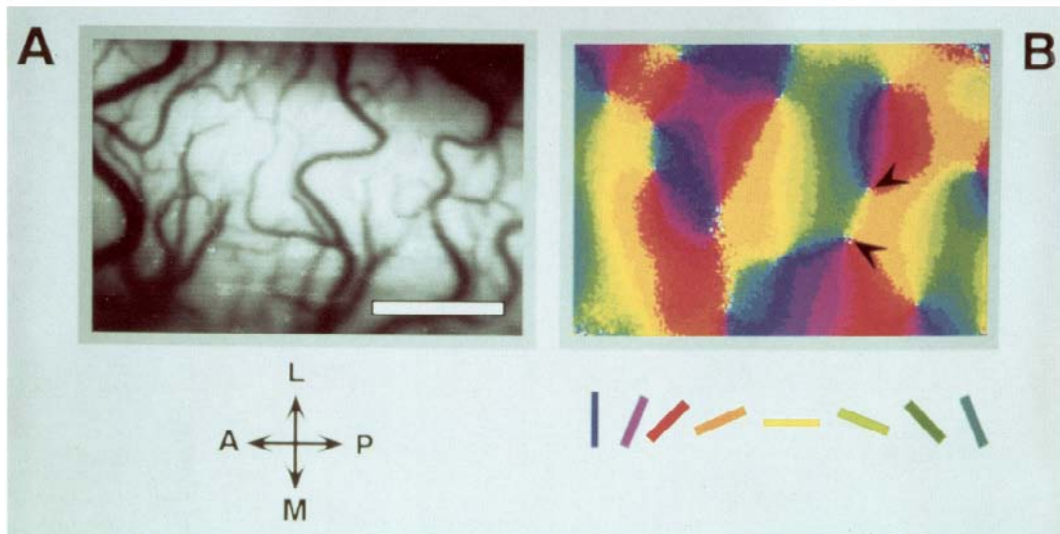


Figure 9. Angle map resulting from vectorial addition of eight single-condition iso-orientation maps. *A*, A picture of the imaged region taken in green light to emphasize the vascular pattern. *B*, Angle map showing the orientation preference for every region of the imaged cortex. For computing the local orientations we took the activity maps obtained with different orientations and added them vectorially on a pixel-by-pixel basis. The angle of the resulting vector is then color-coded according to the scheme at the bottom of the figure: yellow stands for sites responding best to moving gratings of horizontal orientation, regions preferring moving gratings of vertical orientation are coded in blue, and so on. Salient in this map are pinwheel-like structures around orientation centers (arrowheads). Each stimulus was averaged 48 times. No smoothing algorithms were applied. Scale bar, 1 mm.

Figure 3. Correlograms obtained from two cell pairs. *A*, The cell pair had similar receptive properties: The first cell had an orientation preference of 120° , directional preference to the right and an ocular dominance group of 2, the second cell had identical orientation and direction preference and an ocular dominance group of 3. *B*, The first cell was the same cell as the first cell in *A*. The second cell had different receptive field properties: an orientation preference of 20° , upward directionality, and an ocular dominance of 5.

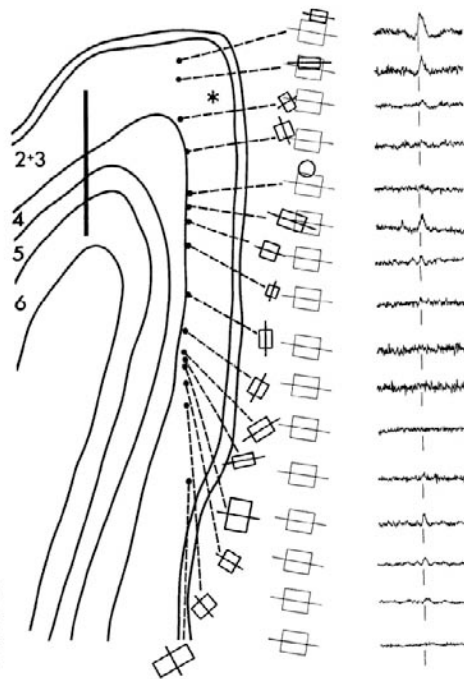
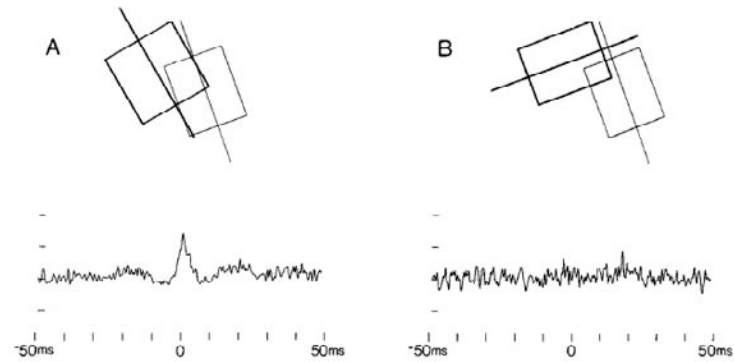


Figure 5. Medial bank penetration similar to Figure 3. Note tendency for the diminishing strength of the peaked correlograms with increases in distance between cells along the medial bank penetration and the reference cell. Also note the large difference in receptive field positions between the recording sites furthest apart.

The general equation for the firing rate of the i -th cell is

$$(3) \quad \tau \frac{dr_i(t)}{dt} + r_i(t) = f \left\{ \frac{1}{N} \sum_j J(\theta_i - \theta_j) r_j(t) + I_{ext}(\theta_i - \theta_0) \right\}$$

where θ_0 is the orientation of the external stimulus, I_{ext} is the input from the sensors, and $f\{\dots\}$ is the nonlinear gain function, *e.g.*, $f\{\mu\} = (1/2)[1 + \tanh(\mu)]$. For convenience we take the continuum limit, *i.e.*, $N \rightarrow \infty$ and $\frac{1}{N} \sum \rightarrow \frac{1}{\pi} \int$, to write the dynamics in terms of the network and external inputs:

$$(4) \quad \tau \frac{dr(\theta, t)}{dt} + r(\theta, t) = f \left\{ \frac{1}{\pi} \int_{-\pi/2}^{\pi/2} d\theta' J(\theta - \theta') r(\theta', t) + I_{ext}(\theta - \theta_0) \right\}.$$

II. Mean field equations

We need to incorporate two approximations to make headway and solve the above set of equations.

The first thing is to specify the interaction and input. We note that in general $J(\theta)$ can be a function of all of the harmonics of θ , *i.e.*, $2\theta, 3\theta$, *etc.* We take the lowest-order, non trivial form and write:

$$(5) \quad J(\theta - \theta') = J_0 + J_1 \cos(\theta - \theta')$$

where we keep the cosine and not the sine term because we expect symmetry with respect to the interaction. Similarly, we take as input to the network only the output of "simple cells", *i.e.*, orientation specific cells, in V1 cortex and write:

$$(6) \quad I_{ext}(\theta - \theta_0) = I_0(t) + I_1(t) \cos(\theta - \theta_0)$$

where θ_0 is the orientation (or phase) of the stimulus. For completeness, input from "complex" cells in cortex would involve terms like $\cos[2(\theta - \theta_0)]$.

The second thing is to form a set of mean-field equations to solve for the $r(\theta, t)$ in a self-consistent manner. Let's go back to the input to the cell with the $f\{\dots\}$ term. The integral can be written:

$$(7) \quad \frac{1}{\pi} \int_{-\pi/2}^{\pi/2} d\theta' J(\theta - \theta') r(\theta', t) = \frac{J_0}{\pi} \int_{-\pi/2}^{\pi/2} d\theta' r(\theta', t) + \frac{J_1}{\pi} \int_{-\pi/2}^{\pi/2} d\theta' \cos(\theta - \theta') r(\theta', t).$$

Recall that $\text{Re} \{e^{i(\theta - \theta')}\} = \cos(\theta - \theta')$. Then:

$$(8) \quad \frac{1}{\pi} \int_{-\pi/2}^{\pi/2} d\theta' J(\theta - \theta') r(\theta', t) = J_0 \frac{1}{\pi} \int_{-\pi/2}^{\pi/2} d\theta' r(\theta', t) + J_1 \text{Re} \left\{ e^{i\theta} \frac{1}{\pi} \int_{-\pi/2}^{\pi/2} d\theta' e^{-i\theta'} r(\theta', t) \right\}.$$

This simplifies in terms of two "order parameters". The mean spike rate at time t is just:

$$(9) \quad r_o(t) = \frac{1}{\pi} \int_{-\pi/2}^{\pi/2} d\theta' r(\theta', t)$$

and the amplitude and phase of the activity modulated by the stimulus is just the complex valued function:

$$(10) \quad r_1(t) \equiv |r_1(t)| e^{-i\psi(t)} = \frac{1}{\pi} \int_{-\pi/2}^{\pi/2} d\theta' e^{i\theta'} r(\theta', t)$$

where the phase is relative to that of the stimulus. So now the interaction simplifies to:

$$(11) \quad \frac{1}{\pi} \int_{-\pi/2}^{\pi/2} d\theta' J(\theta - \theta') r(\theta', t) = J_0 r_0(t) + J_1 \operatorname{Re}\{e^{i\theta} |r_1(t)| e^{-i\psi(t)}\}$$

$$= J_0 r_0(t) + J_1 |r_1(t)| \cos[\theta - \psi(t)] .$$

When all is said and done, the equation for the activity of the neurons becomes:

$$(12) \quad \tau \frac{dr(\theta, t)}{dt} + r(\theta, t) = f\{J_0 r_0(t) + J_1 |r_1(t)| \cos[\theta - \psi(t)] + I_0 + I_1 \cos(\theta - \theta_0)\} .$$

Equations 9, 10 and 12 define the system, to be solved self-consistently.

III. Solution in steady state

Here $dr(\theta, t)/dt = 0$ and thus $r(\theta, t) = r(\theta)$. The equation for the activity becomes

$$(13) \quad r(\theta) = f\{J_0 r_0 + J_1 r_1 \cos(\theta - \psi) + I_0 + I_1 \cos(\theta - \theta_0)\} .$$

Let's assume that the system is linear, that is, all cells are above threshold but not at saturating rates. Then maximizing the right hand side allows us to express the maximum rates, denoted $R(\theta - \theta_0)$, as:

$$(14) \quad R(\theta - \theta_0) = f\{J_0 R_0 + I_0 + (J_1 r_1 + I_1) \cos(\theta - \theta_0)\} .$$

We note that

$$(15) \quad R(\theta - \theta_0) = R_0 + 2R_1(\theta - \theta_0) + \dots$$

by Fourier's Theorem, with the factor of 2 coming from integrating over 2π and not π . Then the linearized equations, *i.e.*, $f\{\mu\} = \mu$, yields:

$$(16) \quad R_0 + 2R_1 \cos(\theta - \theta_0) = J_0 R_0 + I_0 + (J_1 R_1 + I_1) \cos(\theta - \theta_0) .$$

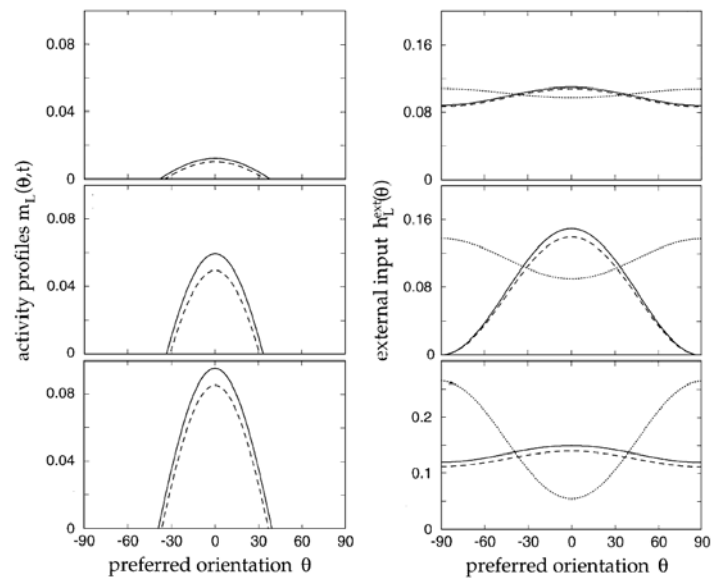
The term that are constant and the terms proportional to $\cos(\theta - \theta_0)$ must each be equated with zero. This leads to a *crux* result:

$$(17) \quad R_0 = \frac{I_0}{1 - J_0}$$

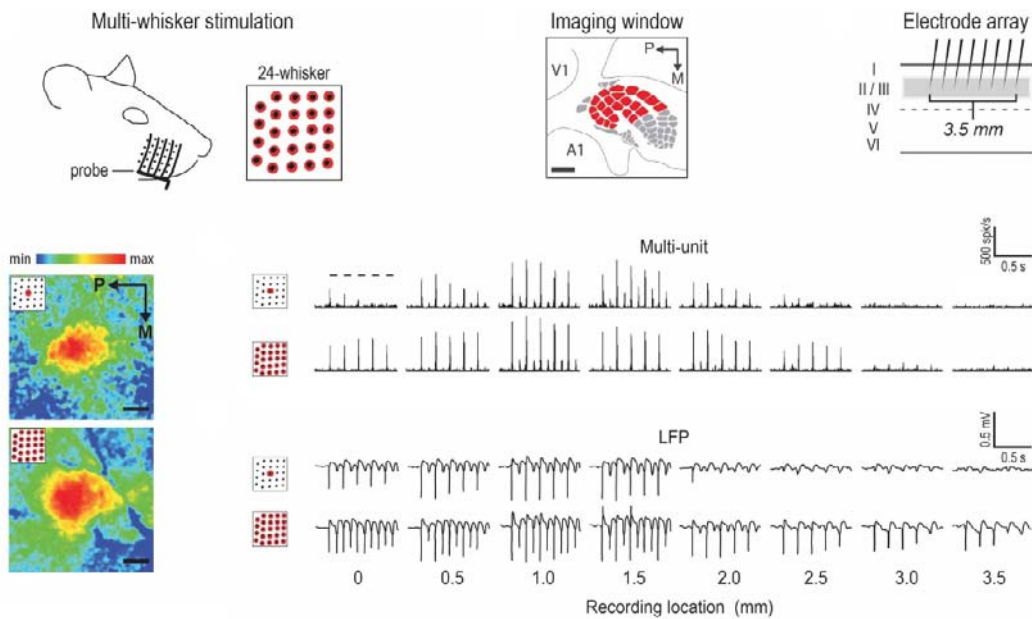
and

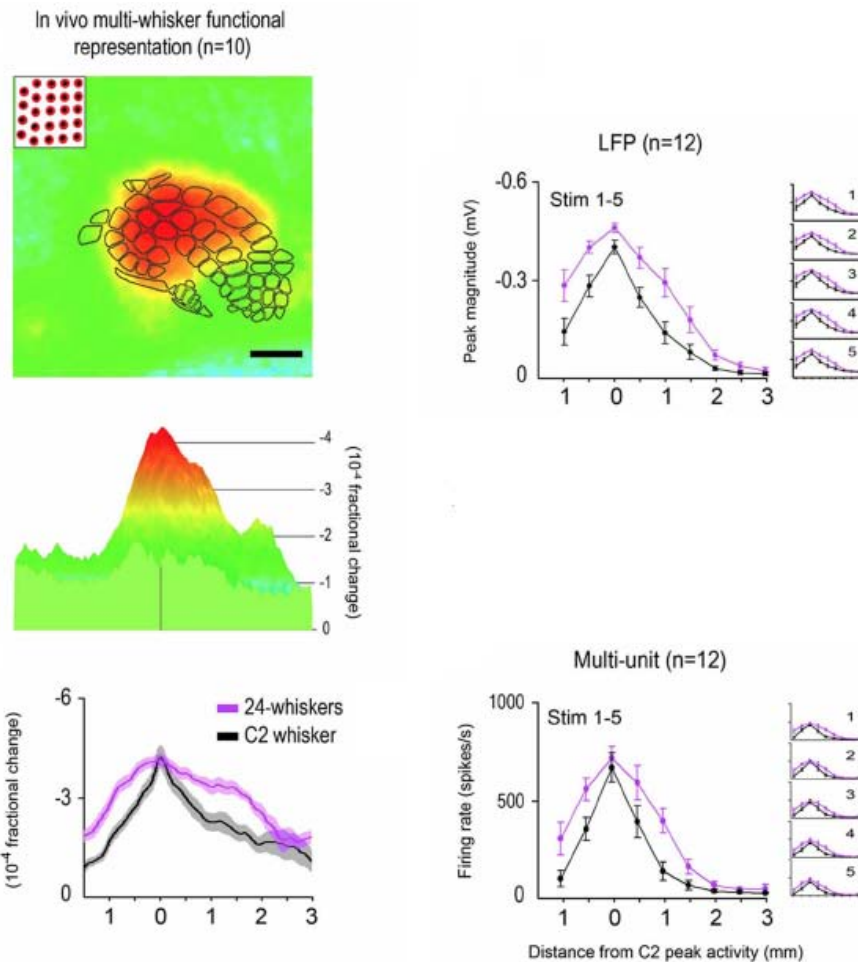
$$(18) \quad R_1 = \frac{I_1}{2 - J_1} .$$

The network amplifies the average rate through the $(1 - J_0)$ term in the denominator and, critically, amplifies the modulation by the $(2 - J_1)$ term. The invariance of the tuning to changes in contrast occurs if the saturating part of full nonlinear form of $f\{\dots\}$ comes into play, so that the output is largely independent of the value of I_1 .



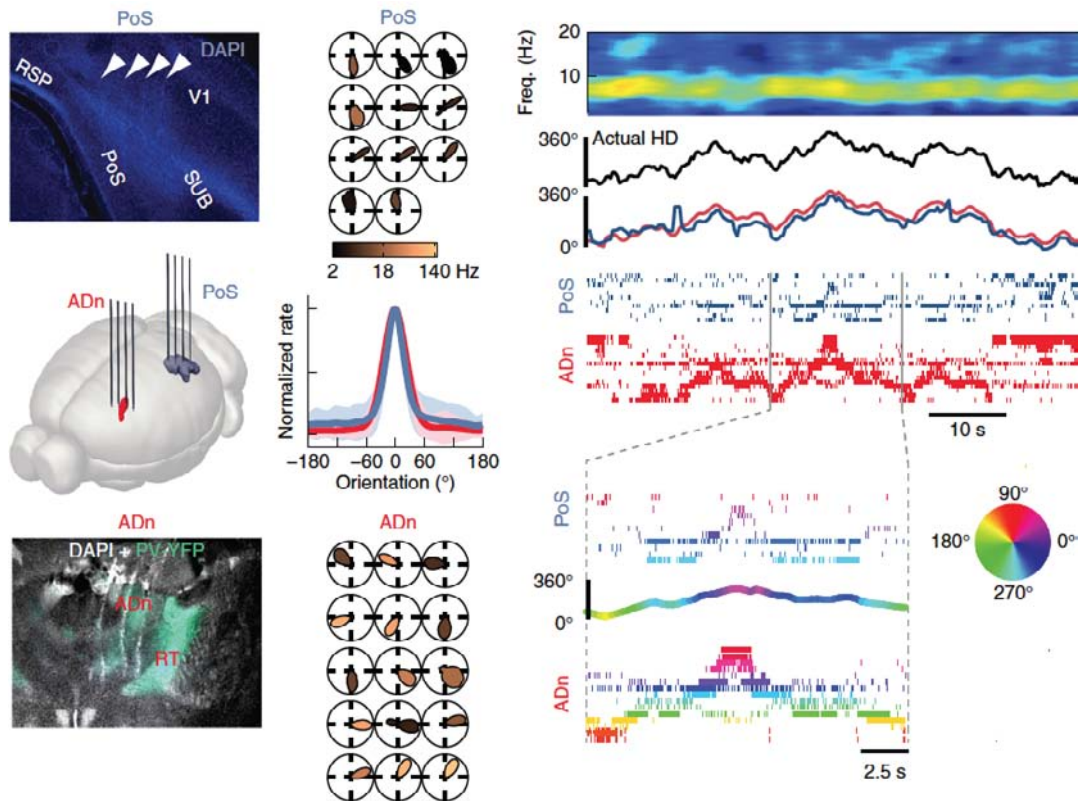
Beyond vision *per se*, amplification may be seen in the very recent data of Frostig (Figures below) on the response of units as well as aggregate measures of neuronal activity in the rat vibrissa system. Stimulation of a single central vibrissa leads to nearly the same spatial extent of activity as stimulation of some 24 vibrissa (center, nearest neighbors, and next nearest neighbors). At the very least the radius of the stimulus is tripled while the width of the response, as judged by the multiunit data, is increase by only some 40 %. This suggests that the cortical response is saturating; whether it is explained by our theoretical mechanism remains to be seen!



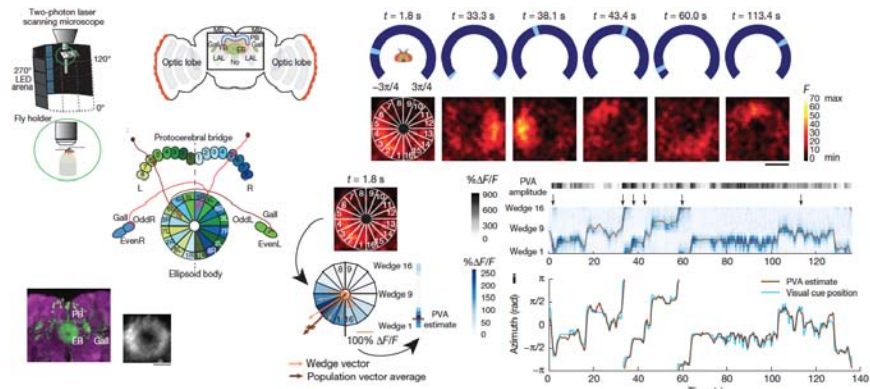


A final point is that the network dynamics get interesting for $J_1 > 2$, which leads to the network picking an arbitrary phase, or drifting through all phases which appear as waves of activity, until the stimulus turns on. This limit can be viewed as a "moving bump" of activity, for which there is evidence from heading in thalamus in mice (see Peyrache Buzsaki 2015) and the ellipsoid body in flies (see Seelig and Jayaraman 2014)

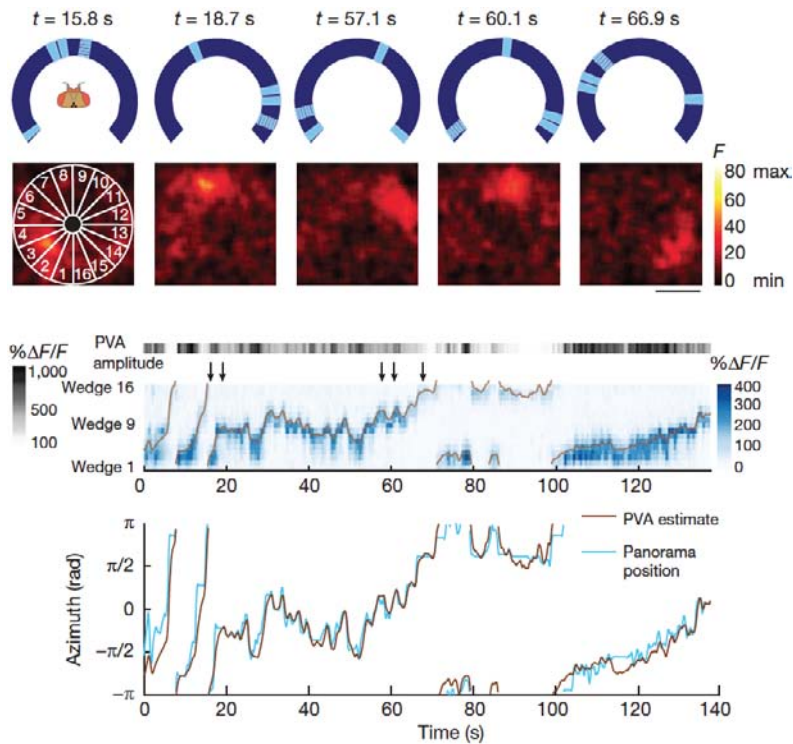
In visual cortex, it is hypothesized that neurons with an orientation preference between the initial and final orientation of the stimulus would be activated. This remains to be seen. A somewhat analogous prediction for activity moving among locations for a visual saccade appears to be observed in the superior colliculus.



Internally organized mechanisms of the head direction sense
 Nature Neuroscience 2015
 Adrien Peyrache, Marie M Lacroix, Peter C Petersen & György Buzsáki



Neural dynamics for landmark orientation and angular path integration
 Nature
 Johannes D. Seelig & Vivek Jayaraman



Neural dynamics for landmark orientation and angular path integration
 Nature
 Johannes D. Seelig & Vivek Jayaraman